Geogr. Fis. Dinam. Quat.
41 (2018). 119-135, 12 figg., 2 tabb.

DOI 10.4461/ GFDQ.2018.41.8

ELIANA VALENZANO [1], GIOVANNI SCARDINO [1, 2], GIULIA CIPRIANO [3], PAOLA FAGO [4], DOMENICO CAPOLONGO [1,2], FRANCESCO DE GIOSA [2], STEFANIA LISCO [1], DANIELA MELE [1], MASSIMO MORETTI [1*] & GIUSEPPE MASTRONUZZI [1,2]

HOLOCENE MORPHO-SEDIMENTARY EVOLUTION OF THE MAR PICCOLO BASIN (TARANTO, SOUTHERN ITALY)

ABSTRACT: VALENZANO E., SCARDINO G., CIPRIANO G., FAGO P., CAPOLONGO D., DE GIOSA F., LISCO S., MELE D., MORETTI M. & MASTRONUZZI G., Holocene *morpho-sedimentary evolution of the Mar Piccolo basin (Taranto, southern Italy).* (IT ISSN 0391-9838,2018).

The Mar Piccolo basin (Gulf of Taranto, northern Ionian Sea) is well-known in literature for the detailed records of Late Pleistocene sea-level changes. The Holocene deposits, however, have never been analysed in detail. In this paper, new geophysical datasets and the data from two wells have been used to investigate the morpho-sedimentary Holocene evolution of this basin. In addition, dating of peat samples and the occurrence of a tephra ("Pomici di Mercato" event – ca 8900 BP) provide the timing of the different evolution stages. Morphological features of the basal unconformity, sedimentological data from core analysis, and the areal distribution of lithofacies have allowed the identification/recognition of an incised-valley system occurrence which had formed during the last sea-level cycle. Furthermore, a polyphasic basal erosional surface, formed during fluvial incision and successive ravinement processes, has been identified. The sedimentary infill records fluvial to transitional environment units of a low energy semi-enclosed basin.

KEY WORDS: Coastal environment, Holocene, incised valley, semi-enclosed basin, Mar Piccolo, Ionian Sea.

RIASSUNTO: VALENZANO E., SCARDINO G., CIPRIANO G., FAGO P., CAPOLONGO D., DE GIOSA F., LISCO S., MELE D., MORETTI M. & MASTRONUZZI G., *Evoluzione morfo-sedimentaria olocenica del bacino del Mar Piccolo (Taranto, Italia).* (IT ISSN 0391-9838,2018).

L'area del Mar Piccolo (Golfo di Taranto, Mar Ionio, Italia meridionale) è nota in letteratura per gli studi sui depositi relativi alle variazioni del livello del mare del Pleistocene superiore. I depositi relativi all'Olocene, invece, non sono mai stati oggetto di studi morfo-stratigrafici di dettaglio. In questo lavoro, nuovi dati geofisici, lo studio della stratigrafia di due pozzi a carotaggio continuo, la datazione di campioni di torba e il riconoscimento di un livello di *tephra* (evento "Pomici di Mercato" - ca 8900 B.P.) hanno permesso di dettagliare le fasi evolutive del Bacino del Mar Piccolo durante l'Olocene. I caratteri geometrici della superficie di *unconformity* basale e la distribuzione latero-verticale delle facies ci ha permesso di interpretare questo bacino come legato all'evoluzione di un sistema tipo *incised-valley*. È stata identificata una superficie erosiva polifasica, formata durante la caduta eustatica e rimodellata durante la risalita del livello del mare. Il riempimento post-glaciale ha uno spessore massimo di circa 30 m e registra la transizione fra depositi alluvionali di piana costiera a unità lagunari e di bacino di transizione di bassa energia.

TERMINI CHIAVE: Ambienti costieri, Olocene, valle-incisa, bacino marino protetto, Mar Piccolo, Mar Ionio.

INTRODUCTION

Coastal sectors are the world's most significant and intensely used areas settled by humans. The analysis of both coastal processes and paleo-environments, has generated a considerable body of literature (i.e. Kay & Alder, 2002; Schwarz, 2005; Anthony, 2009). Coastal areas are sensitive, transitional, morpho-sedimentary systems that respond rapidly to sea-level changes, and that, in the near future, will be subjected to sea-level rises. The duration and magnitude of the relative sea-level changes control: (a) erosional surface occurrence (location and timing), horizontal and vertical shoreline shifts (Posamentier & Allen, 1993;

[1] *Dipartimento di Scienze della Terra e Geoambientali, Università degli Studi di Bari "Aldo Moro", Italy*

[2] *Environmental Surveys S.R.L., Taranto, Italy*

[3] *Dipartimento di Biologia, Università degli Studi di Bari "Aldo Moro", Italy*

[4] *Consorzio Nazionale Interuniversitario per le Scienze del Mare, CoNISMa, Roma, Italy*

**Corresponding author: M. MORETTI, massimo.moretti@uniba.it*

The present study was funded by the Italian Environment Ministry.

We are thankful to the Government Commissioner for the Remediation of the Taranto area (Dr. V. Corbelli) and her collaborators for their financial, logistic, and scientific support in every phase of this project. The authors gratefully acknowledge the Italian Ministry of Education, University and Research (MIUR Funds - PhD in Geosciences, Bari University) and CoNISMa (Project CIG57930987B2 Funds - Responsible M. Moretti). We wish to thank all the staff at the Polo Scientifico e Tecnologico Magna Grecia (Taranto) for the analyses carried out on the cores. We would also like to thank A. Ribolini (Editor) and the three anonymous reviewers for their positive and insightful comments on the first version of the manuscript. Our appreciation also goes to Victoria Sportelli, a native English speaker and lecturer, for the English language revision of the paper.

Catuneanu, 2006; Zecchin & Catuneanu, 2013), and (b) fluvial systems-drainage network changes (Blum & Tornqvist, 2000; Blum & *alii*, 2013). These changes are well-documented and recorded in the sedimentary architecture of marine and transitional areas.

Detailed studies on late Quaternary marine sediments are made possible due to the diffusion and improvement of high-resolution seismic reflection techniques, allowing the mapping of stratigraphically significant surfaces and submerged geomorphological features. Several studies have been conducted in recent years, focusing on the Quaternary evolution of fluvial systems in Central Mediterranean coastal areas (Labaune & *alii*, 2005; Amorosi & *alii*, 2016a). Wide morphological variability and high

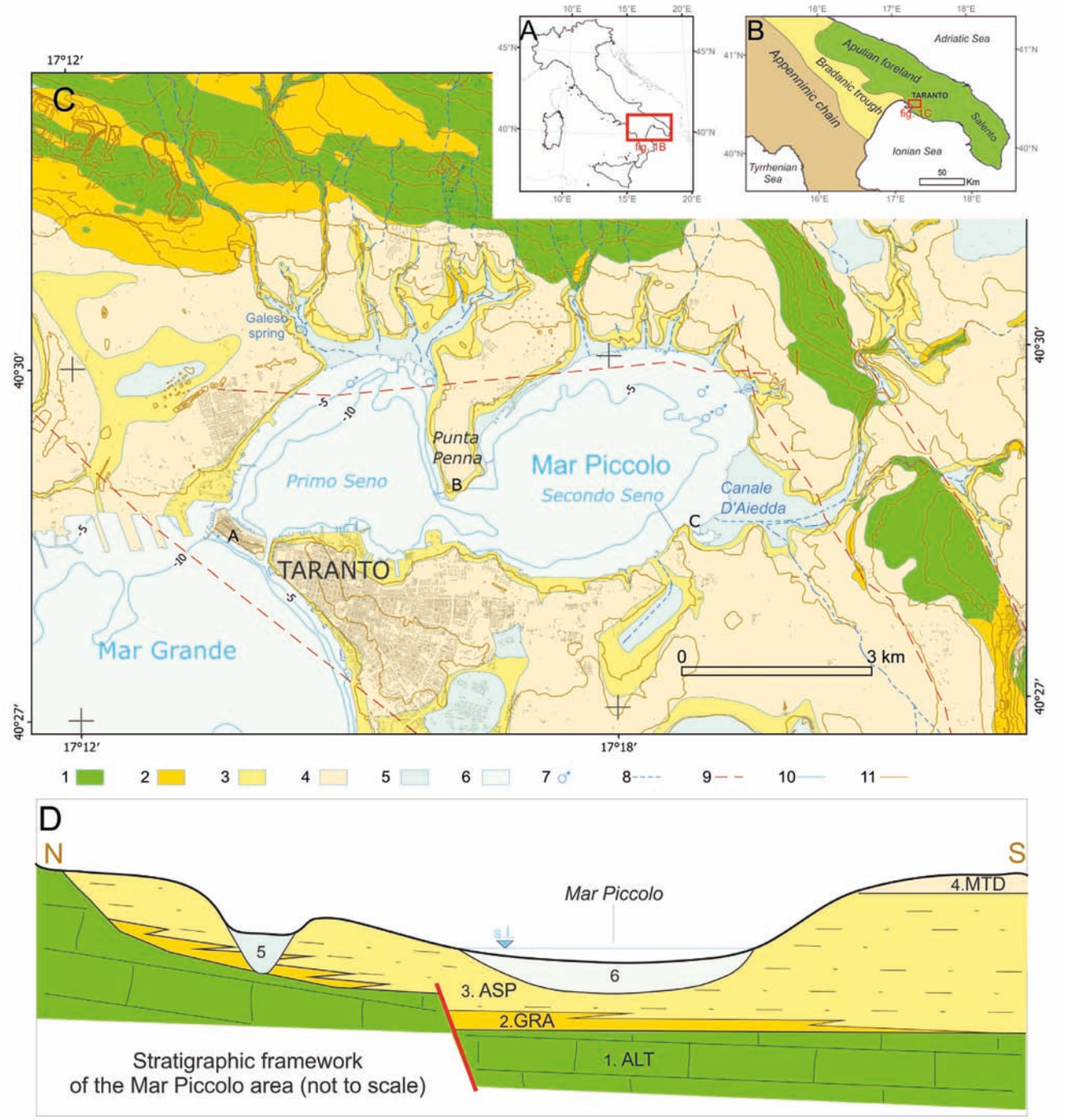

FIG. 1 - A. and B. Location of the study area. C. Geological map, modified after Lisco & *alii* (2016); 1. Calcare di Altamura Fm (Cretaceous); 2. Calcarenite di Gravina Fm (Upper Pliocene - Lower Pleistocene); 3. Argille subappennine informal unit (Pleistocene); 4. Marine terrace deposits (MIS 5); 5. Alluvial deposits; 6. Holocene marine sediments; 7. Submarine springs; 8. Ephemeral drainage networks; 9. Buried faults; 10. Bathymetric contour, every 5 m; 11. Topographic contour, every 10 m. D. Sketch of the geometric relationships between the sedimentary units.

responsiveness to environmental changes have already been documented, highlighting the importance of small rivers sedimentary contribution (Tesson & *alii*, 2005) and their capacity to originate large-scale erosional features during the last relative sea-level fall (Maselli & Trincardi, 2013). Nevertheless, densely-spaced high-resolution seismic data-sets in shallow water are not very common. In fact, large data sets are generally available for the outer shelf (Hernández-Molina & *alii*, 1994; Rabineau & *alii*, 1998; Lericolais & *alii*, 2003; Baztan & *alii*, 2005; Nordfjord & *alii*, 2005). Blum & *alii* (2013) underline that little information is available on channel shapes, processes, and facies in the late Quaternary due to their present submerged state and the core paucity or subsurface data, other than widely-spaced 2D seismic profiles, with few notable exceptions (Rejenstein & *alii*, 2011).

The aim of this study is to unravel the Holocene evolution of an internal sea basin, the Mar Piccolo (Gulf of Taranto, southern Italy), through densely-spaced high-resolution seismic reflection data, validated with two well cores. The Mar Piccolo is a small sheltered basin, partially sealed off from the Ionian Sea by a Pleistocene calcarenite. The catchment basin and the coastal area are both affected by severe environmental issues. Indeed, they host a large city (about 200,000 inhabitants), heavy industries, as well as merchant and military harbours. However, to date, this area has lacked in-depth studies of the submerged geology, seismic data has been limited to a single seismic UNIBOOM profile carried out during the 1980s (Cotecchia & *alii*, 1990), and a geological section constructed to build a bridge across the Mar Piccolo at its narrowest point (i.e.: Cotecchia & *alii*, 1990 and references, therein). Consequently, theories on the Mar Piccolo origin and evolution could not, to date, have been properly supported or validated.

There is no accordance on the genesis of the Mar Piccolo. The quasi-perfect eight-shaped morphology of the Mar Piccolo has been interpreted by some authors as the result of karstic collapses originated in the Mesozoic substrate (De Giorgi, 1922; Parenzan, 1960; Verri & De Angelis D'Ossat, 1899). According to Guerricchio (1988), the presence of depressions in the Taranto area is, related to the anti-clockwise rotation of the Salento area (fig. 1). Pagliarulo & Bruno (1990) suggest that these depressions were induced by tectonic activity involving also the Plio-Pleistocene units. The morphological evolution of the Mar Grande basin (fig. 1) has also been interpreted as having been induced by changes in the drainage network during the Late Pleistocene (Mastronuzzi & Sansò, 1998). The same hypothesis has been extended to the Mar Piccolo (Mastronuzzi & Sansò, 2003; Mastronuzzi & *alii*, 2013). Recently, Guerricchio & Simeone (2013) have interpreted the Mar Piccolo depression as the result of fluidization of the overlaying Plio-Pleistocene sedimentary cover induced by submarine karstic springs, and lateral erosion related to helicoidal vertical flows.

Geophysical data presented in this paper are the first comprehensive high-resolution seismic survey of the area. The exceptional quality and density of the data has allowed: ì) a 2.5 D (pseudo three-dimensional) mapping of the main stratigraphically-significant surfaces, and ìì) the unravelling of the origin and recent evolution of the Mar Piccolo basin. The data set represents part of a larger framework aiming for a complete geo-environmental characterisation. Extensive knowledge of the physical environment is the scientific basis necessary to distinguish natural and anthropic pollution influences, as well as to plan remediation strategies. Finally, furthermore general aims of this study include: ì) a new detailed timing and framework for the evolution of a Holocene coastal system in the Mediterranean area, and ìì) the recognition of main stratigraphic surfaces and their significance in a shallow-water inner basin.

GEOLOGICAL SETTINGS

The Mar Piccolo area (Taranto, southern Italy) is located on the northern Ionian coast, between the south-western sector of the Apulian Foreland and the eastern Bradanic Foredeep. The Apulian Foreland and the Bradanic Foredeep are the Pliocene-Pleistocene foreland/foredeep of the South Apennines orogenic system (Doglioni & *alii*, 1994). The Mar Piccolo basin is separated from the Ionian Sea (Mar Grande area) by a Pleistocene calcarenite peninsula. It is connected with the Mar Grande by two channels; the north-western one is a natural one, while the eastern one was artificially excavated through the Pleistocene calcarenite in the late XIX century (Mastronuzzi & *alii*, 2013). A promontory (Punta Penna) divides the basin into two embayments (Primo and Secondo Seno) creating the eight-shape plan morphology that is characteristic of the Mar Piccolo basin (fig. 1).

The stratigraphy is relatively simple and well-known. Starting from the bottom, it consists of Mesozoic limestone (Calcare di Altamura Fm.), Upper Pliocene-Lower Pleistocene calcarenite (Calcarenite di Gravina Fm.) passing upwards and laterally to the heteropic argille subappennine informal unit (Ricchetti & *alii*, 1988). Marine, transitional, and continental terraced deposits occur in the surrounding foreland and foredeep sectors (Ricchetti, 1967; Ciaranfi & *alii*, 1988). In the Mar Piccolo area, all these sedimentary units crop out and have been recently mapped in detail using mainly the available surface data (Lisco & *alii*, 2016). The landscape is dominated by a series of marine terraces, slightly dipping toward the sea (Ciaranfi & *alii*, 1988) whose deposits unconformably overlay the argille subappennine unit (Mastronuzzi & Sansò, 1998); their age has been inferred from radiometric data ranging from 132 to 116 ka (Dai Pra & Stearns, 1977; Hearthy & Dai Pra, 1992; Belluomini & *alii*, 2002; Antonioli & *alii*, 2008; Amorosi & *alii*, 2014) corresponding to Marine Isotope Substage 5e (= MIS 5.5 - Shackleton, 2000), called "Tyrrhenian" (Issel, 1914; Dépéret, 1918) in the Mediterranean area.

Along the present-day cliffs of the Mar Piccolo basin (fig. 1, fig. 2), the argille subappennine unit continuously crops out; the overlying unconformable marine terraced deposits form a sub-horizontal surface located at a *quasi*-uniform elevation (10-15 m msl), but showing different lithostratigraphic features (Belluomini & *alii*, 2002; Mastronuzzi & *alii*, 2013). Close to the city of Taranto (A in

FIG. 2 - Present-day cliffs in the Mar Piccolo on the east side of Punta Penne (B in fig. 1). The sharp contact between the argille subappennine and the overlying Tyrrhenian (MIS 5e) calcarenites is shown. Present-day erosion induces rock falls in the Tyrrhenian calcarenites and slides in the argille subappennine unit.

fig. 1), a bio-calcarenitic marine terraced unit occurs, reaching its maximum thickness in the peninsula hosting the old city (19 m). This unit passes laterally to coeval sedimentary bodies made up of stunning *Cladocora caespitosa* bioherm cropping out into the Galeso spring area, and close to the *Punta Penne* drawbridge (B in fig. 1) (Peirano & *alii*, 2004; 2009). In the Il Fronte area (C in fig. 1), a marly-sandy unit with specimens of *Persitsistrombus latus* (Gmelin, 1791, = *Strombus bubonius*, Lamark, 1822) and large colonies of *C. caespitosa* occurs: this section has been defined as the Upper Pleistocene global boundary stratotype section and point (GSSP) because it provides an un-interrupted marine sedimentary record of MIS 5e (Antonioli & *alii*, 2008; Amorosi & *alii*, 2014; Negri & *alii*, 2015; Negri & *alii*, 2016).

The Mar Piccolo basin is fed by a complex drainage network of ephemeral streams covering an area of about 500 $km^{2,}$ and by small coastal streams originating from subaerial karst springs. The basin is characterised by a flat sea bottom, reaching a water depth (wd) of 15 m, with some restricted negative anomalies, of up to a 33 m wd. This is related both to the sub-circular depression of submarine karst springs (locally known as "Citri", (Cerruti, 1948; Zuffianò & *alii*, 2015), and to anthropogenic excavations (Lisco & *alii*, 2016).

MATERIAL AND METHODS

Seismic survey

We analysed a densely-spaced network of seismic reflection profiles acquired in 2013 and 2015 by means of two different systems, mounted on board R/V Issel (property of CoNISMa). The first data set consists of 15 km of high-resolution profiles surveyed with a Geo Marine Geo-spark 1000 sparker system, shot with an energy pulse of 350 J and a frequency between 0.2-2 kHz. This system provided a vertical resolution of about 30 cm and a penetration greater than 100 ms (about 50 m below the seabed). The second and largest data set, with a vertical resolution lower than 20 cm, was acquired using an Innomar SES-2000 compact (primary frequency 85-115 kHz) parametric sub-bottom profiler. A total length of 262 km of sub-bottom profiles were recorded owing to the manoeuvrability of the system. This system allowed data acquisition in very shallow water and between the extensive mussel farming structures of the Mar Piccolo (fig. 3). Both data sets were converted into a SEGY format. IXSEA Delph was used to process and interpret the data. Processing steps consisted in converting the acquired data into a SEGY format, frequency filtering, and automatic gain control.

Seismic analysis was based on reflector amplitude, continuity, and lateral terminations (downlap, onlap, toplap, erosional truncation) to recognise key surfaces and seismic units. For the time/depth conversion, an average velocity of 1670 m/s for the sediments, and of 1500 m/s for the water column was used. The average velocity was determined using two cores, and the depth of the key surfaces recognised in the lithological logs was matched with the observed TWT (Two-Way Traveltime) of the key surfaces in the seismic profiles. The dense grid and resolution of the sub-bottom profile data provided a pseudo three-dimensional mapping of the main erosional surface, which were interpolated using ArcGIS Topo to Raster tool.

Core sampling and laboratory analyses

The geophysical data were ground-truthed using a 46 m and a 28 m long cores drilled with a rotary corer mounted on board a barge and retrieved in 1.5 m long and 0.1 m in diameter liners. Following transverse cutting, detailed photos were taken every 20 cm with a camera in a fixed vertical position with an overlap of about 25% with an adjacent photo.

A visual core description was elaborated taking into consideration: degree of the drilling process disturbance; colour (identified using the Munsell soil-colour chart); lithological and granulometric description; sedimentary structures and bedding planes (lamination, granulometric trends); accessories (shell type and proportion of shells and organic material, presence of glauconite or other minerals, concretions and nodules, veins, archaeological findings).

The chronological framework was provided by AMS datings. ^{14}C AMS dating was performed on two peat samples collected at a depth of 25.95 m below the seabed (tab. 1). Measurements were performed at the Centro di Datazione e Diagnostica (CEDAD) Laboratory at the University of Salento (Italy). Absolute dates were calibrated using the

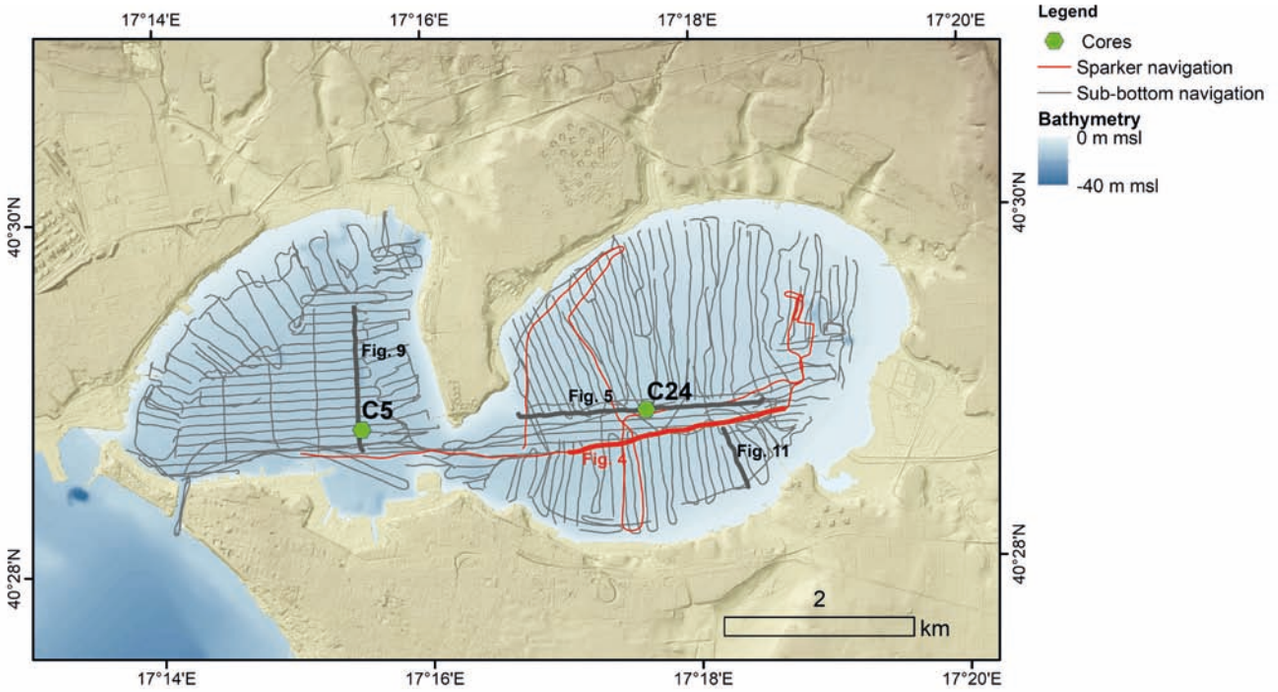

FIG. 3 - Position of the data-sets: in green, the core position; in grey, the sub-bottom profiler track lines; in red, the sparker track lines; thin lines represent all acquired seismic lines and bold lines represent profiles shown in figs. 3, 4, and 9. Coordinates are WGS84.

TABLE 1 - AMS datings and calibration results of peat samples.

ID SAMPLE UNIBA	Depth (m bsb)	ID SAMPLE CEDAD	TYPE	RADIOCARBON AGE (BP)	$\delta^{13}C$	CALIB. CURVE	CAL AGE 1s (%)	CAL AGE 2s (%)
S5BR 25.95	25.95 m	LTL17186A	Peat	9188 ± 75	-8.8 ± 0.2	IntCal 13	BP 10,477-10,471 (0.3)	BP 10,554-10,532 (0.2)
							BP 10,423-10,249 (96)	BP 10,525-10,228 (97)
S5BR 25.95 BIS	25.95 m	LTL17186B	Peat	9255 ± 75	-4.5 ± 0.5	IntCal 13	BP 10,519-10,367 (73)	BP 10,648-10,629 (0.1)
							BP 10,361-10,296 (26)	BP 10,591-10,245 (98)

Calib 7.1 programme (Stuiver & *alii*, 2017). We used the terrestrial radiocarbon calibration curve "IntCal13" for plant material and organic sediment (Reimer & *alii*, 2013). These calibrations yielded ages with 1 and 2 standard deviations (1 sigma, 68.3% confidence level; 2 sigma, 95.4% confidence level). Next to the conventional age range, the relative areas under probability distribution are also provided, in brackets. For each dating, a value of $\delta^{13}C$ was obtained to indicate the origin of the organic matter (Stuiver & Polach, 1977; Wilson & *alii*, 2005).

Finally, we performed component analyses on a 4-20 cm thick tephra level, identified in the cores at 18-19 m below the sea bottom (bsb). Analyses were carried out using a Zeiss-Leo EVO50XVP scanning electron microscope coupled with an X-max (80 mm^2) Silicon drift Oxford detector equipped with a Super Atmosphere Thin Window©; operative conditions were: 15 kV accelerating potential, 500 pA of probe current (corresponding to about 25,000 output cps on Co standard), counting time 50 s and 8.5 mm working distance. X-ray intensities were converted into oxides using the XPP model for matrix corrections, developed by Pouchou & Pichoir (1988; 1991), and granted as software support by Oxford-Link Analytical (UK). Microanalytical data were checked using reference standards from Micro-Analysis Consultants Ltd (UK); analytical precision was 0.5% for concentrations > 15 wt.%, 1% for concentrations of about 5 wt.%, and < 15% for concentrations near the detection limit.

RESULTS

Seismo-stratigraphy

Seismic analysis highlighted the presence of two key seismic horizons (Horizon A and Horizon B, fig. 4) which, together with the seabed, form the boundaries of three main seismic units (S1, S2, S3, fig. 4).

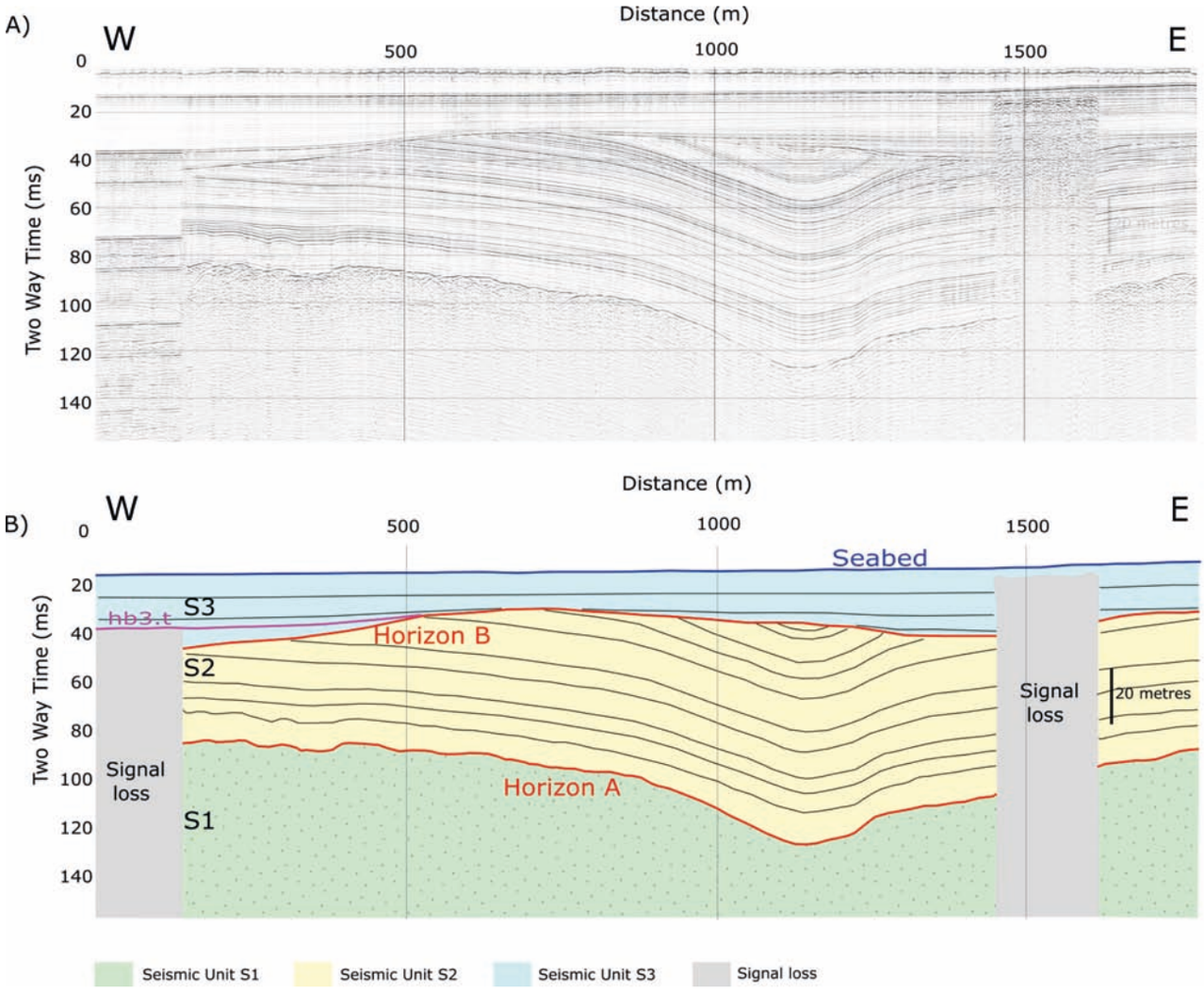

FIG. 4 - A. Uninterpreted Sparker profile; B. Interpretation of profile showing: areas of signal loss (grey); chaotic Seismic Unit S1 (green); Seismic Unit S2 (yellow) with parallel reflections; Seismic Unit S3 (light blue) with onlapping sub-horizontal reflections and continuous internal reflection horizon hb3.t (purple line); erosional surfaces in red (Horizon A and Horizon B); location of core C24 (fig. 7) in black; position of the profile displayed in figs. 3 and 6.

SEISMIC UNIT S1. The deeper Seismic Unit, named S1, represents the acoustic basement in the sparker profiles. It is bounded on top by Horizon A (fig. 4). Unit S1 is marked by high-amplitude chaotic and discontinuous reflections, and can be interpreted as a hard substratum.

Horizon A is visible only in the sparker profiles from about 29 m up to 82 m below the seabed (bsb) and constitutes a key stratal surface between Seismic Unit S1 and the overlying S2. It has a rough irregular unconformity, detected only in the sparker profiles, showing some local gentle depressions.

SEISMIC UNIT S2. At the bottom, Seismic Unit S2 is delimited by Horizon A, and at the top, by Horizon B. It appears as a well-layered seismic facies with continuous medium amplitude reflectors draping Horizon A (fig. 4). The internal stratification, visible with remarkable detail in the sparker profile (fig. 4), is generally sub-parallel, with some very smooth folding. Reflectors are truncated and terminate by toplap below Horizon B. Parametric sub-bottom profiles show a consistent decrease in signal penetration in correspondence to this unit, seemingly suggesting a substratum which is harder than the overlying Seismic Unit S3 (fig. 5).

Horizon B is the unconformity between the on-lapping reflectors of Seismic Unit S3 and the truncated reflectors of S2 (fig. 5). It represents an uneven surface, deepening towards the central part of the two sub-basins, up to a maximum depth of about 40 m bsb (52 m below msl – fig. 6). This unconformity is visible in the entire dataset and is affected by signal blanking in its deepest portion.

The Horizon B DEM (with 10 x 10 m cell), created using an iterative finite difference interpolation technique (Arc GIS, Topo to Raster tool), shows a complex concave-up surface marked by a sinuous E-W elongated topographic low (fig. 6). Horizon B can be interpreted as an erosional basin-wide unconformity.

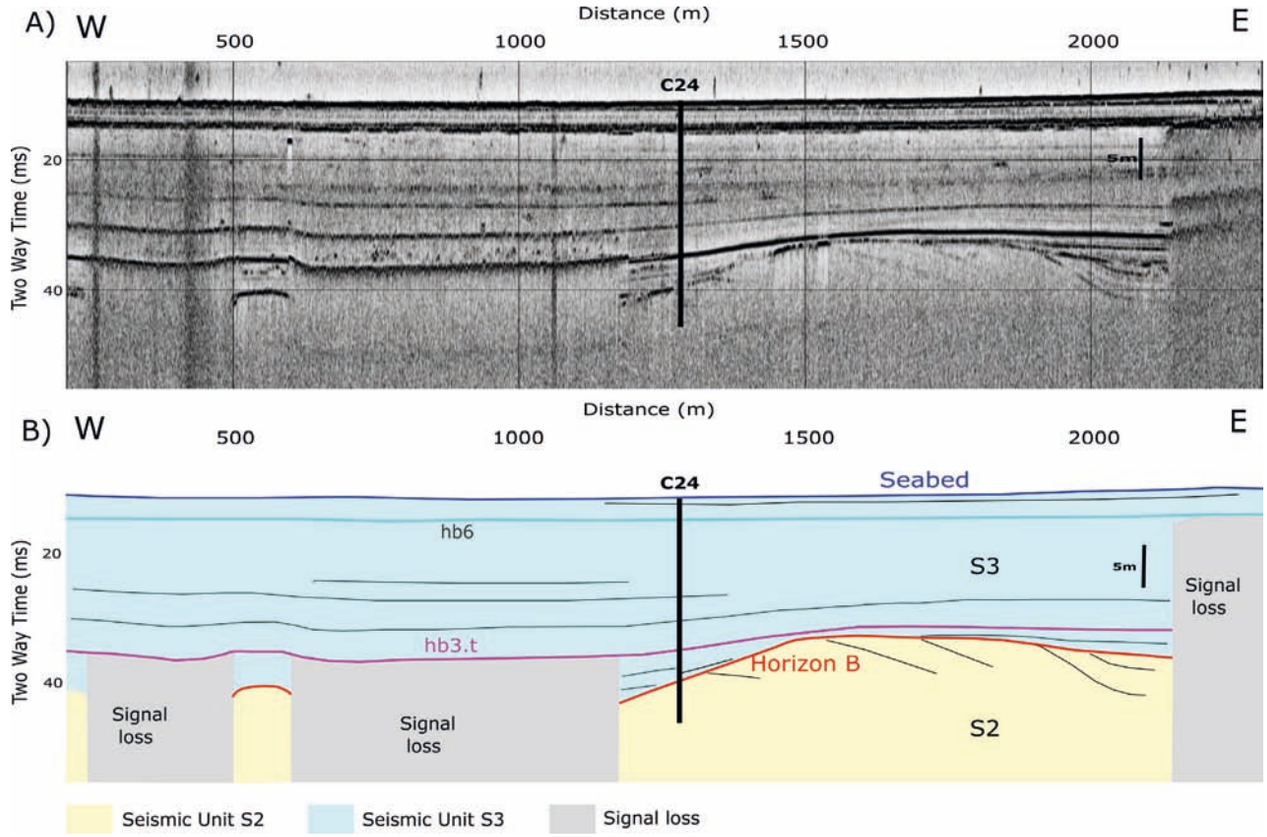

FIG. 5 - A. Uninterpreted Sub-bottom profile; B. interpretation of profile showing uppermost Seismic Unit S2 with reflections truncated by horizon B (red); Seismic Unit S3, internal continuous reflectors hb3.t (purple line) and hb6 (light blue line); areas of signal loss (grey); location of core C24 (fig. 7) in black; position of the profile displayed in figs. 3 and 6.

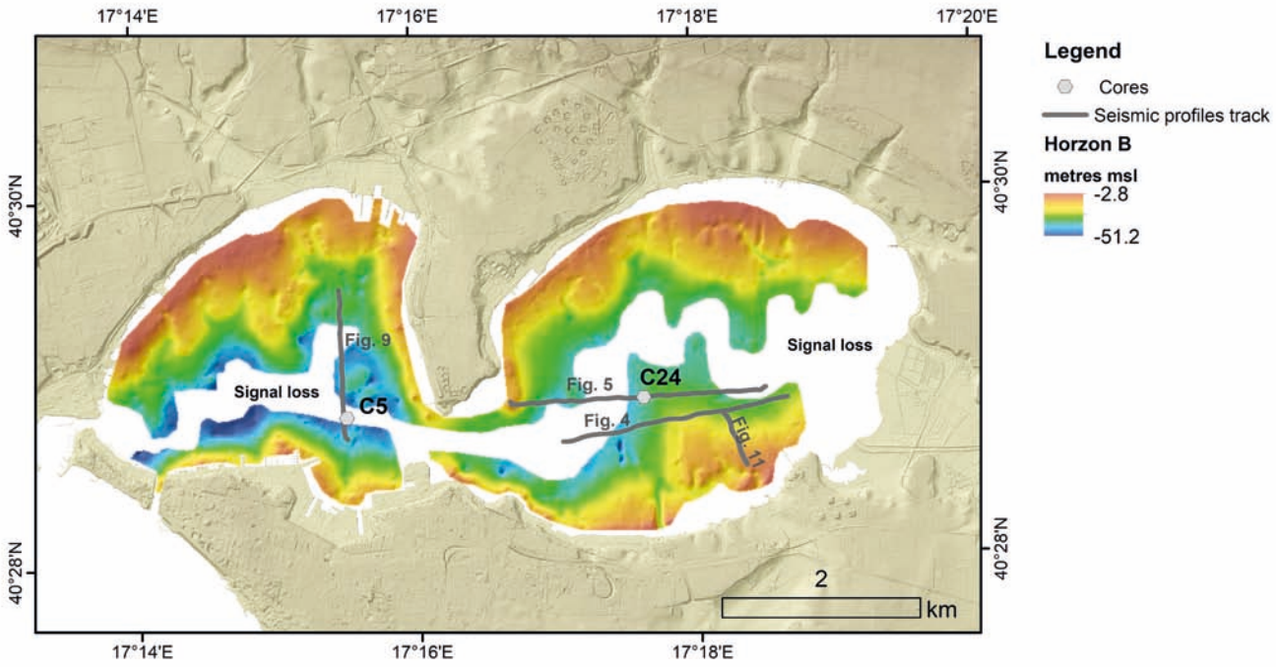

FIG. 6 - DEM of the interpolated surface corresponding to the horizon B erosional surface, depth is in metres below mean sea-level, velocity used for conversion: 1500 m/s for seawater, 1670 m/s for sediments. Note the presence of a sinuous area of signal loss in the deepest part of the surface.

TABLE 2 - Major oxide (%) concentration in the glass from the Pomici di Mercato Tephra. Mean and standard deviation values for 16 EDS analyses are shown.

Oxide	Oxide%	St. Dev.
SiO_2	59.68	0.72
Al_2O_3	20.91	0.29
Na_2O	7.63	1.01
K_2O	7.20	0.41
FeO	1.90	0.15
CaO	1.89	0.17
MnO	0.12	0.12
TiO_2	0.03	0.07
MgO	0	0
TOT	99.36	0.04

SEISMIC UNIT S3. S3 is the uppermost seismic unit and has a lenticular geometry with a thickness of up to 40 m. It is bounded by Horizon B at the bottom and by the seabed on the top. It is a layered seismic unit with few high-amplitude sub-horizontal, slightly concave-up reflectors ranging from low to high amplitude, with onlap terminations on Horizon B. It constitutes the infilling of the Horizon B surface. The extremely high penetration of the seismic signal suggests that S3 is composed of soft muds (figs. 4 and 5).

The upper part of S3 is marked by a reflector at a depth of 5-16 m bsb, with very high amplitude and continuity; it is named Horizon hb6 (light blue in fig. 5). This reflector, parallel to the seabed, is interpreted as the lower limit of more recent, coarser, and less consistent sediments.

In the lower part of S3, the main reflector is Horizon hb3.t, visible at an average depth of 18-19 m. Horizon hb3.t is a high-amplitude, continuous reflector. It is responsible for most of the signal-masking effects occurring in the central part of the basin, diagnostic of sediments with a high fluid content.

Sedimentary Units and datings

On the basis of lithological features, biological content, and stratigraphic position, two main stratigraphic units were distinguished in the cores: ASP and H (fig. 7). They correspond, respectively to the S2 and S3 seismic units (tab. 3).

UNIT ASP - Unit ASP consists of a greenish, marly, silty clay with millimetric laminations, and occasionally containing organic matter. The colour varies from pale olive green to greenish grey with brownish (locally reddish) mottles related to iron-oxides. Oxidised sediments are located just below the unconformable surface between the ASP and H units.

This lithofacies is extremely stiff. Its pocket penetrometer values range from 7.5 kg/cm^2, in the lower part, to 4.5 kg/cm^2, in the upper part, close to the unconformable surface. The bioclastic content consists of very small marine fauna shell fragments (<2mm) as well as abundant calcareous nanno-fossils and foraminifera (mainly *Globigerina bulloides*, *Globorotalia inflate,* and *Globigerinoides ruber*). The ASP was observed both in core C24, starting from a depth of 22 m bsb, and in core C5, from 42 m bsb (fig. 7).

The ASP unit shows the lithostratigraphic characters of the argille subapennine informal unit (Cilumbriello & *alii*, 2010; "argille del Bradano" in Martinis & Robba, 1971). This can be easily correlated to the outcrops constituting the cliffs surrounding the Mar Piccolo (fig. 2). We have interpreted the brownish-reddish mottles and lower stiffness at the upper boundary of the ASP as being related to sub-aerial exposure and weathering.

UNIT H - It consists of a succession starting from the bottom of three lithofacies (Ha, Hp, Hb).

The lower lithofacies, Ha, abruptly overlies the Unit ASP (fig. 7). It consists of coarse, yellowish-brownish beds and firm sandy mud intercalations of a pale olive green colour. Coarser beds are composed of poorly sorted sand and gravel with abundant bioclastic debris containing a mélange of reworked remains of marine bivalves, marine and pulmonate gastropods, *C. caespitosa* fragments. Muddy levels contain some sand laminations, bioclast fragments, diagenetic carbonatic nodules, reddish mottles due to iron oxides, and occasionally dark spots of organic matter. In core C5, Ha begins with coarse, poorly-sorted gravel deposits, consisting of decimetric calcareous pebbles and

TABLE 3 - Correlation of seismic units with sedimentary units

Seismic Unit - Horizon	Sedimentary Unit	Lithofacies	Lithology
Seismic Unit S3	H	Hb	structureless very soft silts with abundant organic content and bioclasts
Horizon hb3.t		tephra	"Pomici di Mercato" whitish volcanic ashes
Seismic Unit S3		Hp	alternation of clayey silts with *C. glaucum* and peat beds with pulmonate gastropods
		Ha	alternation of sand to gravel beds with limestone-calcarenite pebbles and firm sandy mud with reworked remains of *C. caespitosa*
Seismic Unit S2	ASP	ASP	alternation of marly silt, shale and fine sand

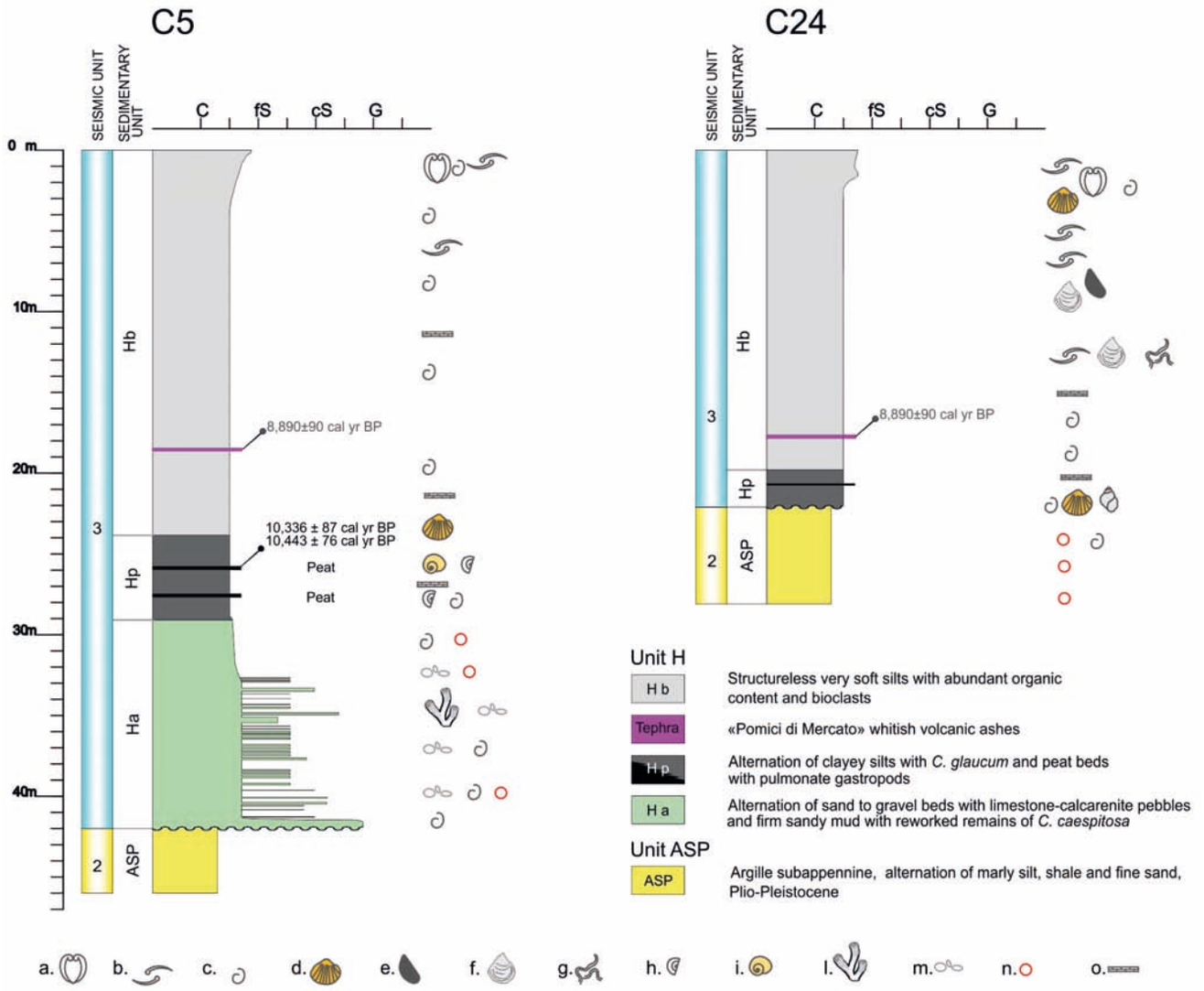

FIG. 7 - Sedimentary units of core C5 and C24 with indication of estimated grain size, lithological accessories and correlation to seismic units. Datings of Pomici di Mercato tephra are taken from Mele et al. (2011). Peat datings are reported in tab. 1. Key: a - articulated bivalves, b - disarticulated valves; c - unspecified marine mollusc fragments; d - *Cerastoderma glaucum*; e - *Mytilus* spp.; f - Ostreidae.; g - Polychaeta spp.; h - pulmonate gastropod fragments; i - pulmonate gastropods; l - *Cladocora caespitosa* fragments; m - carbonatic nodules; n - Iron oxides/hydroxides; o - organic matter. Position of the cores in figs. 3 and 6.

bioclastic debris. Gradually, this basal gravel interval passes upwards to alternations of coarse sand and silt with rare clasts of the underlying ASP unit. Pocket penetrometer values measured on the silt levels are approximately 2 kg/cm^2. The lithofacies in C5 has a thickness of 13 m, while, in core C24, it is not observed.

Ha can be interpreted as the result of deposition in the subaerial settings. Fluvial incision and alluvial processes seem to be responsible for the high-energy facies of this unit. Coarser-grained transported material comes from the erosion of the older outcropping units: *C. caespitosa* fragments (from MIS 5e terrace deposits), siltstone clasts (from the argille subappennine), limestone, and calcarenitic pebbles (from the Calcare di Altamura Fm and Calcarenite di Gravina Fm, respectively).

Ha gradually passes upwards to Hp (core C5, fig. 7). In core C24, Hp unconformably lies on the ASP Unit, at a depth of 22 m, and is marked by a sharp change in colour and sediment stiffness.

Generally, Hp is a 4-5 m thick interval of grey clayey silts intercalated with peat beds. Grey silts are very soft, organic-rich, and marked by the presence of well-preserved specimens of *Cerastoderma glaucum*. Peat beds are composed of plant remains (mainly *Phragmites australis*), abundant and

well-preserved ostracods, and pulmonate gastropod shells (*Helix* sp., *Rumina* sp., *Pomatias* sp. and the dominant taxon *Planorbis* sp.), few reworked fragments of marine bivalves and gastropods, and foraminifera. The plant remains of a peat level at a depth of 26 m below the seabed, were radiocarbon dated, yielding an age of about 10.4 ka (tab. 1).

The absence of carbonate concretions and oxides in the Hp lithofacies marks the transition from oxidizing to reducing conditions, and is indicative of a paralic environment. Alternations of peat levels with *Planorbis* sp. and silts with *C. glaucum* represent small oscillations between a low-energy swamp environment and a lagoon environment.

Hp gradually passes to the upper lithofacies, Hb. This consists of very soft, grey, structureless silts with an abundant organic content and bioclasts. Hb contains well-preserved broken shells and millimetric fragments of mainly marine gastropods and bivalves.

The lower part of Hb is composed of homogenous clayey silts with only millimetric shell fragments. This part contains a 4-20 cm thick tephra level, at 18-19 m bsb level in both cores C5 and C24.

An increased bioclastic content and particle size are present at the top, up to 3-4 m below the present-day water-sediment interface; here, it is easy to distinguish marine gastropods (*Bolinus brandaris, Bittium* sp.), scaphopoda (*Antalis inaequicostata*, "*Dentalium*" sp.), as well as abundant bivalves (*Acanthocardia paucicostata, Corbula gibba, Mytilus galloprovincialis, Ostrea edulis*).

The uppermost interval is a very loose, organic-rich sandy silt, strongly affected by both the drilling disturbance and intense anthropic activity, such as mussel farming, anchoring, fishing, and marine infrastructures in the area.

Hb deposited in a semi-enclosed basin with low hydro-dynamicity, from a restricted to the larger present-day semi-enclosed basin: it is the result of transgression and continuous vertical aggradation.

A whitish tephra layer was identified in the Hb lithofacies, at about 18 m below the seabed. It is 12-15 cm thick and is composed of fine to coarse ash. The tephra layer stands out as a light-grey layer, with a high-porosity (and high-water content), very low bulk density, and a very soft

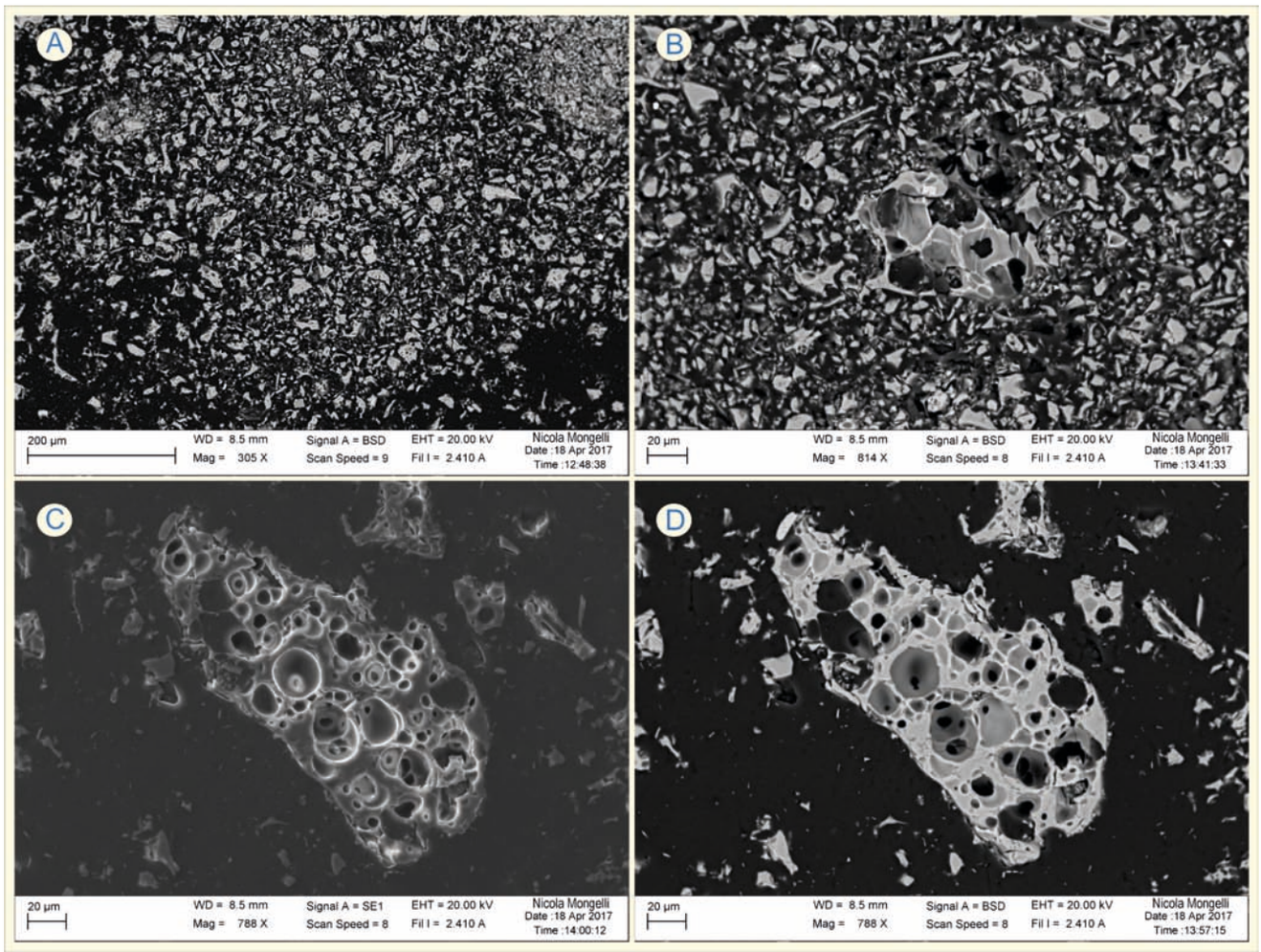

FIG. 8 - SEM Images of the tephra layer occurring in cores C5 and C24. In figs. 8.A and 8.B, the tephra layer seems to be composed totally of glass shards with fine to coarse ash dimensions. In figs. 8.C and 8.D, BSD and secondary electron images are shown. Note the presence of circular vesicles.

consistency. Lamination is not well-visible, but it is generally marked by some thin, grey, silty laminae. Main petrographical features were observed using an optical binocular microscope: the tephra is composed of volcanic mainly transparent glass particles, and rarely whitish or grey; loose crystals are represented predominantly by femic minerals occurring as brownish euhedral crystals. To better describe the tephra particle morphology and evaluate the glass compositional features, the tephra layer were sampled in the 2 cores (4 samples in every core). A total of 8 samples were analysed using a scanning electron microscope (SEM) along with energy dispersive spectrometer (EDS) analyses. The entire layer is composed of glass shards and highly vesicular fragments with spherical and sub-spherical vesicles (fig. 6). An EDS analysis was performed on individual glass particles to establish the major element compositions. 16 EDS analyses (2 for each sample) were obtained. They showed a constant phonolithic composition of the glass particles: SiO_2 is about 60%, Al_2O3 about 21%, Na_2O and K_2O about 7.5%, CaO and FeO about 2% (tab. 2). The closest source of volcanic materials having these compositional features is the Somma-Vesuvius area where, during the last 20 ka, many high-energy Plinian and sub-Plinian events have occurred (Santacroce, 1987; Cioni & *alii*, 2008). In detail, the tephra colour, the glass composition, and the stratigraphic position are compatible with the Pomici di Mercato event, dated 8890±90 cal yr BP, (Aulinas & *alii*, 2008; Mele & *alii*, 2011).

Seismic unit correlation with well cores results

CARBONATE SUBSTRATUM - The acoustic basement (Seismic Unit S1) can be easily attributed to the Calcare di Altamura Fm (Upper Cretaceous) and the Calcarenite di Gravina Fm (Upper Pliocene-Lower Pleistocene): they are compact carbonate units cropping out in the emerged adjacent areas.

ARGILLE SUBAPPENNINE - Seismic Unit S2 corresponds to the argille subappennine informal unit sampled at the bottom of the cores (ASP Unit in fig. 7). High values of stiffness, recorded with a pocket penetrometer, result in medium-amplitude reflectors in the sparker record. Furthermore, well-layered sub-horizontal reflectors correspond to the metric alternations between the arenaceous and marly portions of this informal unit described in literature (Casnedi, 1988).

EROSIONAL SURFACE - Core analysis results show a correlation of this surface with the abrupt contact between the sedimentary Unit ASP and the Unit H. In core C5, the erosional limit is marked by the overlying alluvial gravel of the Ha lithofacies (42 m bsb); in the sub-bottom profiles, these coarse-grained deposits locally mask the basal erosional surface (see chapter Late Pleistocene - Holocene sequence; fig. 9)

In core C24, the same erosional surface coincides with the contact of the Hp coastal swamp-lagoon sediments on the argille subappennine (22 m bsb), corresponding, in the sub-bottom profiles, to the clearly visible unconformity between the truncated S2 reflectors and the onlapping S3

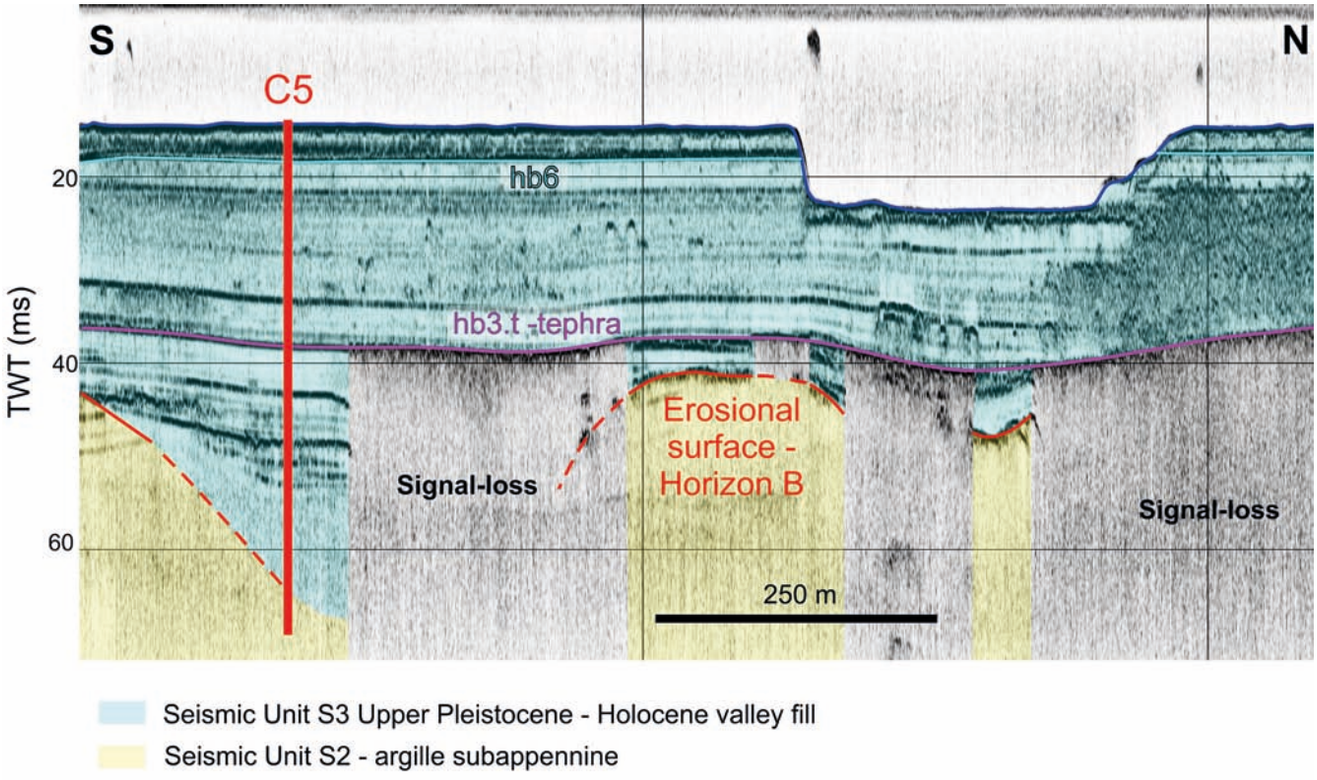

FIG. 9 - Interpreted sub-bottom profiler close to core C5. The depression on the right in the picture corresponds to a large excavation built in the 1920s to recover the large hull of a sunken military ship.

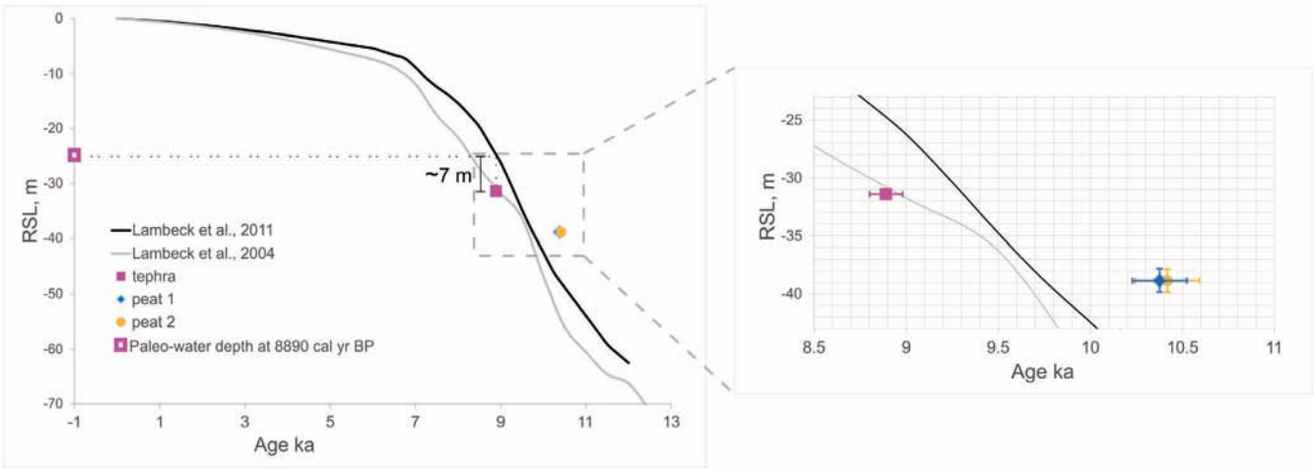

FIG. 10 - Time constraints compared with the Lambeck sea-level curves for the Taranto area; tephra (in pink), below Lambeck & *alii* (2011) curve is compatible with deposition in a very shallow marine environment, the position of peat level (orange) above the two curves is in accordance with the deposition in a transitional environment.

reflectors (Horizon B, fig. 5). Therefore, the depth of the erosional surface is consistent with both the seismic and core data.

Furthermore, the interpolated surface (DEM in fig. 6) clearly shows a sinuous and ribbon-shaped course which is in agreement with the subaerial hydrographic pattern. On the other hand, the deeper part of this complex surface is covered by alluvial gravel deposits which are visible in core C5: all the data reveal a deep fluvial influence in the general morphology of this unconformity.

This incision can be considered the intermediate sector of a larger fluvial system (Mastronuzzi & Sansò, 1998) including the present-day landward stream Canale D'Aiedda, and the elongated seaward depression visible in the Mar Grande.

LATE PLEISTOCENE - HOLOCENE - Seismic Unit S3 is associated with the entire Unit H. This unit represents the sedimentary infill of the erosional surface. It consists of the lithofacies Ha subaerial-fluvial deposits, Hp lagoon muds, and Hb shallow marine muds.

In greater detail, we can correlate the signal attenuation areas, signal loss, and reflectors hb3.t and hb6 to specific sedimentary features recognised in the cores:

– signal attenuation, recognisable close to the erosional surface, seems to be related to the presence of the coarser and stiffer lithofacies Ha;
– signal loss below Reflector hb3.t matches perfectly with the depth of the tephra layer (Ht). The exceptionally high porosity of the tephra is responsible for fluid accumulation and can cause a quasi-complete reflection of the acoustic signal. The sinuous area of blanking in the erosional surface DEM may be due to the thicker tephra deposits present in the sinuous and elongated basin depocenter (figs. 6 and 9).

The tephra layer shows an unexpected thickness that might be due to redeposition. Furthermore, it is prone to fluid accumulation due to its porosity. Water or biogenic gas might accumulate in the bathymetrically lower part of the basin. Fluid-gas charge sediments are common in the shallow stratigraphic record (Judd & Hovland, 1992), and it has also been verified that the tephra layer in marine settings can have a high hydraulic conductivity (Harders & *alii*, 2010).

DISCUSSION

The results of the present study provide evidence of the existence of an incised-valley (or paleovalley *sensu* Blum & *alii*, 2013). The erosional surface forms an elongated topographic low (Zaitlin & *alii*, 1994) that truncates older strata (Zaitlin & *alii*, 1994; Posamentier, 2001). The valley is filled with a sedimentary sequence (Unit H) recording a landward migration of the lithofacies (Van Wagoner & *alii*, 1988; Dalrymple & Zaitlin, 1994).

The sedimentary architecture of the Mar Piccolo shows the typical framework of valleys incised and filled during the last eustatic cycle. In detail, the Unit H facies distribution records the vertical transition from a swamp to a lagoon (Hp lithofacies) during a transgressive stage, as described, on a larger scale, in the Arno (Rossi & *alii,* 2011; Amorosi & *alii,* 2013*;* Sarti & *alii,* 2015) and Po plains (Amorosi & *alii,* 2016b; Campo & *alii,* 2017). On the other hand, the predominance of shallow marine sediments (lithofacies Hb) is comparable to the framework of paleovalley fills in the Japan lowlands (Ishihara & *alii,* 2012*;* Tanabe & *alii,* 2015).

Preliminarily, it can be assumed that the erosional surface incision and subsequent infill (Unit H) are post MIS 5e in age due to the occurrence of abundant *C. caespitosa* remains found in the Ha unit, and indicative of the cannibalisation of the Tyrrhenian reefs.

The age of the infill is considered to be predominantly Holocene. This has been established on the basis of the following two main time constraints:

– peat level in core C5, yielding an age of about 10.3 ka;
– tephra layer identified as the Pomici di Mercato eruption (8890±90 cal yr BP).

The two time-constraints were compared with the Lambeck & *alii* (2004; 2011) sea-level curve available also for Taranto area (fig. 10). The curve is a predictive model taking into account the eustatic change and spatially variable glacio-hydro-isostatic response (Lambeck & *alii*, 2004), and has been calibrated with biological, sedimentological, erosional, and archaeological sea-level indicators. It refers to the present-day mean sea level, and is a recognised tool for the study of paleo-water depth and shoreline location in the area. More specifically, the peat level is considered as a good sea-level marker (Vacchi & *alii*, 2016). Indeed, it represents a coastal environment, and, in the cores, it is immediately preceded and followed by levels containing *C. glaucum.* This Lamellibranchia lives in Mediterranean lagoons up to a depth of about -2 m (Lambeck & *alii*, 2004; Ferranti & *alii*, 2006). Therefore, the dated peat level is considered to have formed in a coastal swamp close to the sea-level, and, in accordance with its position, above the Lambeck & *alii* (2004; 2011) sea-level curve (fig. 10).

The Lambeck & *alii* (2011) sea-level curve was also used to infer the paleo-water depth during the Pomici di Mercato eruption (8890±90 cal yr BP). At that time, the predicted sea-level (based on the curve) was -25 m msl (fig. 10), while the top of the tephra layer was found at an average depth of -32.4 m msl (19 m bsb), thereby suggesting that the volcanic ashes deposited in a very shallow basin (at a depth of about 6-7 m). According to this hypothesis, the top of the tephra layer can provide a good approximation of the paleo-bathymetry at the time of deposition.

The age of the lower time constraint (peat level) of the Mar Piccolo paleo-valley infill shows that fluvial (and sub-aerial) erosion in the MP paleo-valley system culminated during the Last Glacial Maximum, similarly to several other paleo-valleys in the Mediterranean and French Atlantic coasts (Billeaud & *alii*, 2005; Chaumillon & *alii*, 2010; Tropeano & *alii*, 2013; Maselli & Trincardi, 2013; Amorosi & *alii*, 2016a; Ruberti et *alii*, 2017; Ruberti & *alii*, 2018). Nevertheless, the mapped and reconstructed erosional unconformity could not be the result of just fluvial processes. As pointed out by Strong & Paola (2008), incised valleys evolve continuously throughout both sea-level fall and rise, producing erosional surfaces that are highly diachronous and amalgamated; the basal erosional unconformity forms over most of the duration of the sea-level cycle and does not represent a topographic surface. Furthermore, according to Cattaneo & Steel (2003), when sedimentary records corresponding to a relative sea-level lowstand are not preserved, at the base of the transgression there might be a complex polygenetic surface which originated from subaerial erosion during times of a relative sea-level lowstand (a sequence boundary) and subsequent reworking during the ensuing transgression.

In the case of the Mar Piccolo, a clear fluvial origin can be detected from the mapped erosional surface, even though the present-day sub-circular shape of the Mar Piccolo cannot be interpreted only as the result of fluvial incision.

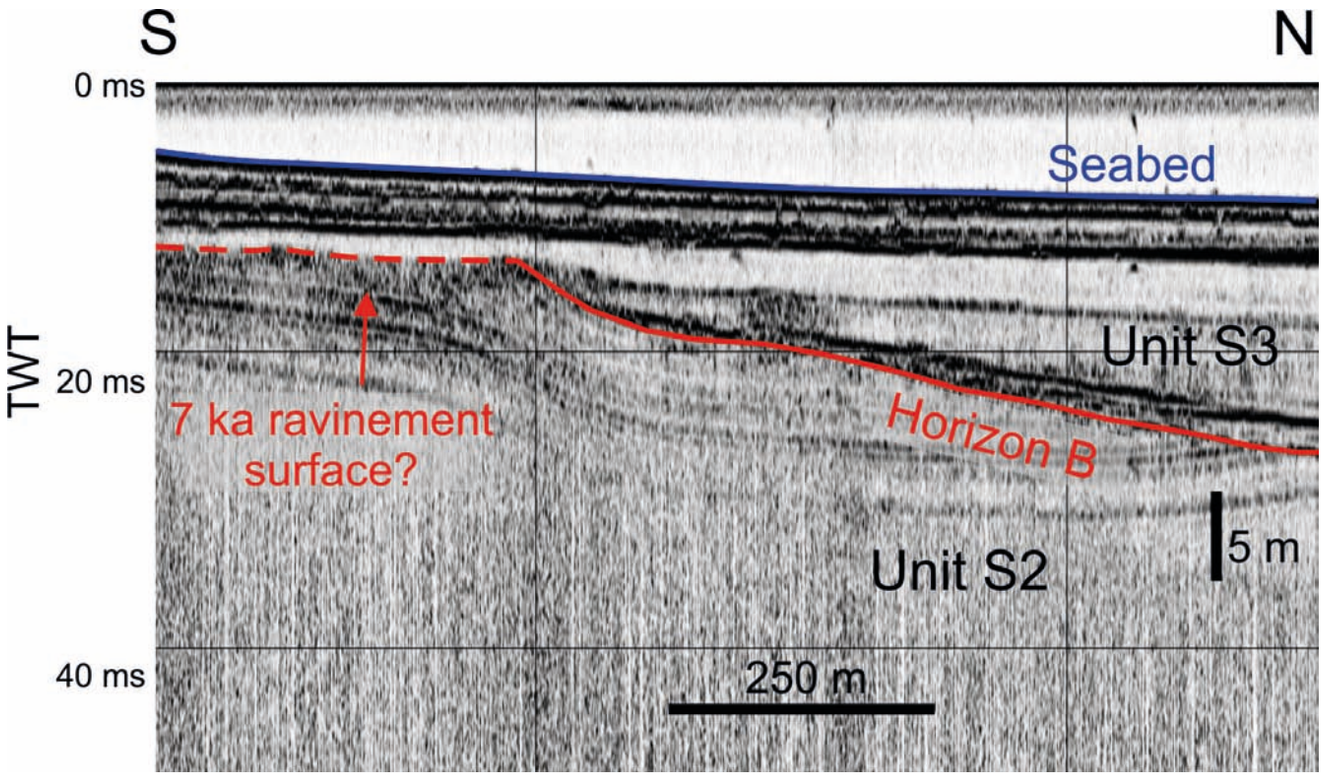

FIG. 11 - Sub-bottom profile showing a change in slope along Horizon B, where the flat portion is interpreted as a wave ravinement surface. Profile track position in fig. 5.

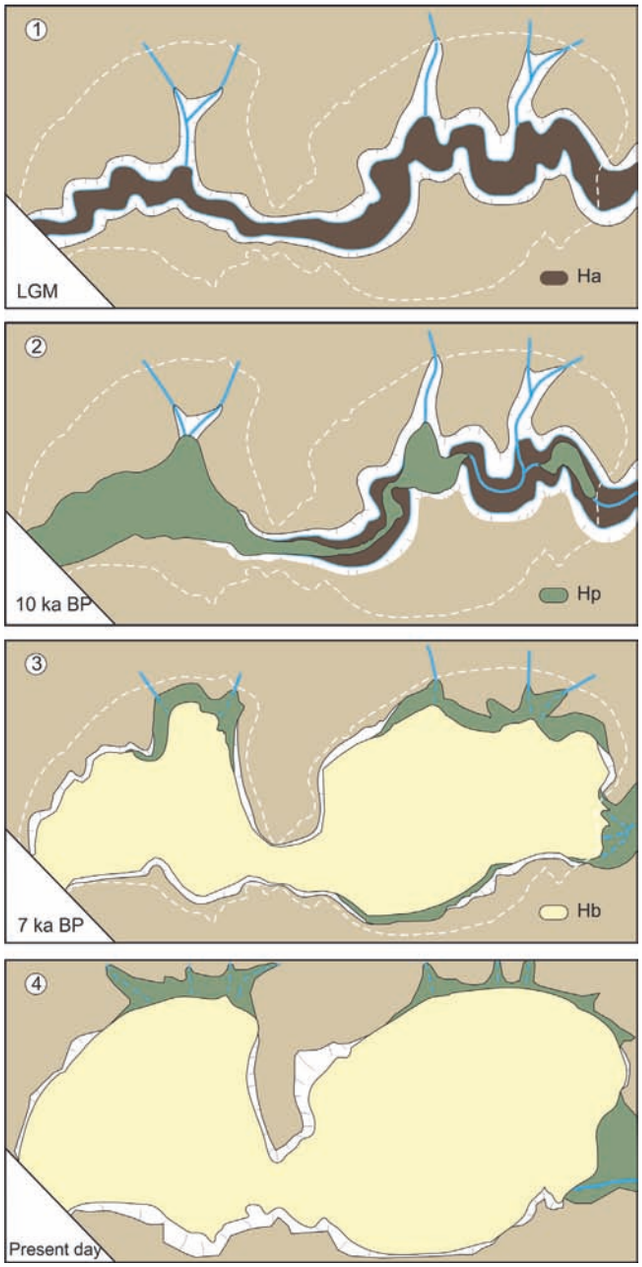

FIG. 12 - Sketch of the morpho-sedimentary evolution of the Mar Piccolo basin. 1. Fluvial incision and deposition of alluvial/continental deposits of lithofacies Ha (brown); 2. deposition of paralic facies Hp (green) and beginning of marine ingression; 3. Deposition of lithofacies Hb (yellow) during transgression; 4. Basin widening and shoreface retreat during sea-level stillstand.

In the Mar Piccolo, the present hydrodynamic conditions are characterised by a semi-diurnal tide regime with a range of about ± 0.2 m (Armenio & *alii*, 2016; 2017), while average wave height is around 0.3 m (Mossa, 2017; Armenio & *alii*, 2017) with the most frequent incoming direction confined to NNE/SSW.

Despite the low-energy hydrodynamic conditions, wave and tide erosions strongly affect the cliffs surrounding the Mar Piccolo due to the high erodibility of the cliff lithology (fig. 2).

We argue that the shoreface processes retreated due to wave and tide ravinements which had occurred during the transgression, when the Mar Piccolo fluvial incision was flooded, forming a ria (*sensu* Evans & Prego, 2003 and references, therein). The same processes probably culminated during the slowing down of sea-level rise (from 8-7 ka), causing the widening of the erosional surface.

In the stratigraphic record, on a larger scale, the processes of wave and tide ravinements affecting and modifying the basal unconformity during transgressive phases are common (Posamentier & Allen, 1993; Cattaneo & Steel, 2003; Chaumillon & *alii*, 2010; Zecchin & *alii*, 2011), and, in some cases, according to the Bruun law, are responsible for shoreface retreat according to the Bruun law (Bruun, 1962; Swift, 1968; Bruun, 1983).

Furthermore, some flat portions of Horizon B, visible in some sub-bottom profiles at a depth of -8, -9 m msl (fig. 11), suggest that a cliff retreat occurred during the slowing down of the sea-level rise (about 7 ka), according to the model of Zecchin & *alii* (2011) and the Lambeck & *alii* (2011) sea-level curve (fig. 10).

CONCLUSION

High-resolution seismic reflection surveys, core analyses, and absolute datings allowed the detection and investigation of the erosional surface nature of the Mar Piccolo, shedding new light on the morpho-sedimentary evolution after the MIS 5.

The main finding of this study is related to the origin of the Mar Piccolo basin. We have documented, for the first time ever, that the present-day flat seabed of the Mar Piccolo hides a basin-wide erosional unconformity buried under a thick cover of Late Pleistocene - Holocene sediments. Our data show that the Mar Piccolo evolution can be interpreted as result of the erosional and depositional processes in transitional low-energy settings of an incised-valley system during last sea-level cycle. Through the features of a ria, the present-day circular perimeter of the two Mar Piccolo embayments is the result of the recent and present-day continuous landward retreat of the highly erodible cliffs.

More specifically, we have documented the interplay of fluvial incisions and reduced-magnitude wave - tide ravinement actions on the polyphasic erosional surface, as well as the genesis of a low-energy semi-enclosed basin acting as a sediment sink.

Taking into account the temporal constraints obtained with absolute datings, the erosive/sedimentary evolution of this basin can be traced as follows (fig. 10):

– Post MIS 5e – beginning of fluvial incision of marine terraced deposits and underlying argille subappennine unit;
– MIS 2 – Last Glacial Maximum (LGM); deposition of alluvial high-energy facies (Ha);
– ~10 ka – beginning of marine ingression in the Mar Piccolo area and formation of a ria; deposition of Hp

facies in coastal freshwater swamp environment; rapid sea-level rise, increase in sediment accommodation and deposition of a thick, semi-enclosed low-hydrodynamic succession (Hb).

– 8.9 ka – deposition of tephra in semi-enclosed settings;
– 7/8 ka to present day – slowing-down of the sea-level rise, erosion of the coastal portions, cliff retreat, widening of the erosional unconformity, and contemporaneous deposition in low-energy and shallow water setting (from a lagoon to the larger present-day semi-enclosed basin).

REFERENCES

Amorosi A., Bini M., Giacomelli S., Pappalardo M., Ribecai C., Rossi V., Sammartino I. & Sarti G. (2013) - *Middle to late Holocene environmental evolution of the Pisa coastal plain (Tuscany, Italy) and early human settlements.* Quaternary International, 303, 93-106. doi: 10.1016/j.quaint.2013.03.030.

Amorosi A., Antonioli F., Bertini A., Marabini S., Mastronuzzi G., Montagna P., Negri A., Rossi, V., Scarponi D., Taviani M., Angeletti L., Piva A. & Vai G.B. (2014) - *The Middle-Upper Pleistocene Fronte Section (Taranto, Italy): An exceptionally preserved marine record of the Last Interglacial.* Global and Planetary Change, 119, 23-38.

Amorosi A., Bracone V., Campo B., D'Amico C., Rossi V. & Rosskopf C. M. (2016a) - *A late Quaternary multiple paleovalley system from the Adriatic coastal plain (Biferno River, southern Italy).* Geomorphology, 254, 146-159. doi: 10.1016/j.geomorph.2015.11.023.

Amorosi A., Bruno L., Campo B., Morelli A., Rossi V., Scarponi D., Hong W., Bohacs K.M. & Drexler T.M. (2016b) - *Global sea-level control on local parasequence architecture from the Holocene record of the Po Plain, Italy*. Marine and Petroleum Geology 1-13. doi: 10.1016/j.marpetgeo.2017.01.020.

Anthony E.J. (2009) - *Shore processes and their paleoenvironmental applications*. Developments in Marine Geology 4, 519 pp.

Antonioli F., Deino A., Ferranti L., Keller J., Marabini S., Mastronuzzi G., Negri A., Piva A., Vai G.B. & Vigliotti L. (2008) - *Lo studio della sezione "Il Fronte" per la definizione del piano Tarantiano (Puglia, Italy).* Il Quaternario, Italian Journal of Quaternary Sciences, 20 (2), 31-34.

Armenio E., Ben Meftah M., Bruno M.F., De Padova D., De Pascalis F., De Serio F., Di Bernardino A., Mossa M., Leuzzi G. & Monti P. (2016) - *Semi enclosed basin monitoring and analysis of meteo, wave, tide and current data*. EESMS 2016 - 2016 IEEE Workshop on Environmental, Energy, and Structural Monitoring Systems, Proceedings 7504835.

Armenio E., De Serio F. & Mossa M. (2017) - *Analysis of data characterizing tide and current fluxes in coastal basins*. Hydrology and Earth System Sciences 21 (7), 3441-3454.

Aulinas M., Civetta L., Di Vito M. A., Orsi G., Gimeno D. & Fér-nandez-Turiel J.L. (2008) - *The "Pomici di mercato" Plinian eruption of Somma-Vesuvius: magma chamber processes and eruption dynamics*. Bullettin of Volcanology 70, 825-840.

Baztan J., Berné S., Olivet J.L., Rabineau M., Aslanian D., Gaudin M., Réhault J.P. & Canals M. (2005) - *Axial incision: The key to understand submarine canyon evolution (in the western Gulf of Lion).* Marine and Petetroleum Geology 22, 805-826. doi: 10.1016/j.marpetgeo.2005.03.011.

Belluomini G., Caldara M., Casini C., Cerasoli M., Manfra L., Mastronuzzi G., Palmentola G., Sanso P., Tuccimei P. & Vesica, P.L. (2002) - T*he age of Late Pleistocene shorelines and tectonic activity of Taranto area, southern Italy*. Quaternary Science Review, 21, 525-547.

Billeaud I., Chaumillon E. & Weber O. (2005) - *Evidence of a major environmental change recorded in a macrotidal bay (Marennes-Oleron Bay, France) by correlation between VHR seismic profiles and cores.* Geo-Marine Letters, 25, 1-10. doi. 10.1007/s00367-004-0183-0.

Blum M., Martin J., Milliken K. & Garvin M. (2013) - *Paleovalley systems: Insights from Quaternary analogs and experiments*. Earth-Science Reviews, 116 (1), 128-169.

Blum M.D. & Tornqvist T.E. (2000) - *Fluvial responses to climate and sea-level change: A review and look forward*. Sedimentology, 47, 2-48.

Bruun P. (1962) - *Sea level rise as a cause of shore erosion*. Journal of the Waterways and Harbors Division, 88 (1) 117-130.

Bruun P. (1983) - *Review of conditions for uses of the Bruun Rule of erosion*. Coastal Engineering, 7 (1), 77-89.

Campo B., Amorosi A. & Vaiani S.C. (2017) - *Sequence stratigraphy and late Quaternary paleoenvironmental evolution of the Northern Adriatic coastal plain (Italy).* Palaeogeography. Palaeoclimatology, 466, 265-278. doi: 10.1016/j.palaeo.2016.11.016.

Casnedi R. (1988) - *La Fossa bradanica: origine, sedimentazione e migrazione*. Memorie della Società Geologica Italiana, 41, 439-448.

Cattaneo A. & Steel R. J. (2003) - *Transgressive Deposits: a review of their variability*. Earth Science Reviews, 62, 187-228. doi: 10.1016/S0012-8252(02)00134-4.

Catuneanu O. (2006) - *Principles of sequence stratigraphy*. Elsevier, 386 pp.

Cerruti A. (1948) - *Le sorgenti sottomarine (Citri) del Mar Grande e Mar Piccolo di Taranto*. Annali Istituto Superiore Navale Di Napoli, Napoli, VII, 171-196.

Chaumillon E., Tessier B., & Reynaud J. Y. (2010) - *Stratigraphic records and variability of Incised valleys and estuaries along French coasts*. Bulletin de la Société Géologique de France, 181 (2), 75-85. doi: 10.2133/gssgfbull.181.2.75.

Ciaranfi N., Pieri P. & Ricchetti G. (1988) - *Note alla carta geologica delle Murge e del Salento (Puglia centromeridionale)*. Memorie della Società Geologica Italiana, 41, 449-460.

Cilumbriello A., Sabato L., Tropeano M., Gallicchio S., Grippa A., Maiorano P., Mateu-Vicens G., Rossi, C.A., Spilotro G., Calcagnile L. & Quarta G. (2010) - *Sedimentology, stratigraphic architecture and preliminary hydrostratigraphy of the Metaponto coastal-plain subsurface (Southern Italy)*. In: Bersezio R. & Amanti A. (Eds.), Proceedings of the National Workshop "Multidisciplinary approach for porous aquifer characterization", Memorie descrittive della Carta Geologica d'Italia XC, 67-84.

Cioni R., Bertagnini A., Santacroce R. & Andronico D. (2008) - *Explosive activity and eruption scenarios at Somma-Vesuvius (Italy): towards a new classification scheme*. Journal of Volcanology and Geothermal Research, 178, 331-346. doi: 10.1016/j.jvolgeores.2008.04.024.

Cotecchia F., Lollino G., Pagliarulo R., Stefanon A., Tadolini T. & Trizzino R. (1990) - *Hydrogeological conditions and field monitoring of Galeso submarine spring in the Mar Piccolo of Taranto (southern Italy).* 11th Proceeding of Salt water intrusion meeting: Gdansk, 171-208.

Dai Pra G. & Stearns C. E. (1977) - *Sul tirreniano di Taranto. Datazioni su coralli con il metodo del 230Th/ 234U*. Geologica Romana, 16, 231–242.

Dalrymple R.W. & Zaitlin B.A. (1994) - *High-resolution stratigraphy of a complex, incised valley succession, Cobequid Bay – Salmon River, Bay of Fundy, Canada*. Sedimentology, 41, 1069-1091.

De Giorgi C. (1922) - *Descrizione geologica e idrografica della Provincia di Lecce*. R. Tipografia, Ed. Salentina, Lecce, 498 pp.

Dépéret C. (1918) - *Essai de coordination chronologique generale des temps quaternaires*. Comptes Rendus de l'Accademie des Sciences 167, 418-422.

Doglioni C., Mongelli F. & Pieri P. (1994) - *The Puglia uplift (SE Italy): An anomaly in the foreland of the Apenninic subduction due to the buckling of a thick lithosphere*. Tectonics, 13 (5), 1309-1321.

Evans G. & Prego R. (2003) - *Rias, estuaries and incised valleys: is a ria an estuary?* Marine Geology, 196, 171-175. doi: 10.1016/S0025-3227(03)00048-3.

Ferranti L., Antonioli F., Mauz B., Amorosi A., Dai Pra G., Mastronuzzi G., Monaco C., Orrù P., Pappalardo M., Radtkei U., Pietro R., Romano P., Sansò P. & Verrubbi V. (2006) - *Markers of the last interglacial sea-level high stand along the coast of Italy: Tectonic implications*. Quaternary International, 145-146, 30-54. doi: 10.1016/j.quaint.2005.07.009.

Guerricchio A. & Simeone V. (2013) - *Caratteri geologico-strutturali dell'area di Taranto e potenziali implicazioni sulla genesi del Mar Piccolo di Taranto (Puglia)*. Tecniche per la difesa dall'inquinamento-34° Corso di Aggiornamento, Guardia Piemontese (CS) Italy.

Guerricchio, A. (1988) - A*spetti geologici sull'evoluzione dei litorali e loro influenza nel campo geologico-applicativo*. Geologia Applicata e Idrogeologia, 23, 29-78.

Harders R., Kutterolf S., Hensen C., Moerz T. & Brueckmann W. (2010) - *Tephra layers: A controlling factor on submarine translational sliding?,* Geochemistry, Geophysics, Geosystems, 11 (5), 1-18. doi: 10.1029/2009GC002844.

Hearty P.J. & Dai Pra G. (1992) - *The age and stratigraphy of Middle Pleistocene and younger deposits along the Gulf of Taranto (Southeast Italy)*. Journal of Coastal Research 8 (4), 882-905.

Hernández-Molina F., Somoza L., Rey J. & Pomar L. (1994) - *Late Pleistocene-Holocene sediments on the Spanish continental shelves: Model for very high resolution sequence stratigraphy*. Marine Geology 120, 129–174. doi: 10.1016/0025-3227(94)90057-4.

Ishihara T., Sugai T. & Hachinohe S. (2012) - *Fluvial response to sea-level changes since the latest Pleistocene in the near-coastal lowland, central Kanto Plain, Japan*. Geomorphology 147-148, 49-60. doi: 10.1016/j.geomorph.2011.08.022.

Issel A. (1914) - *Lembi fossiliferi quaternari e recenti nella Sardegna meridionale*. Accademia Nazionale dei Lincei, ser. 5, 23, 759-770.

Judd A. G. & Hovland M. (1992) - *The evidence of shallow gas in marine sediments*. Continental Shelf Research, 12 (10), 1081-1095.

Kay R. & Alder J. (2002). - *Coastal planning and management*. Taylor & Francis, 387 pp.

Labaune C., Tesson M. & Gensous B. (2005) - *Integration of High and Very High-resolution Seismic Reflection Profiles to Study Upper Quaternary Deposits of a Coastal Area in the Western Gulf of Lions, SW France*. Marine Geophysical Researches, 26 (2-4), 109-122. doi: 10.1007/s11001-005-3711-z.

Lambeck K., Antonioli F., Anzidei M., Ferranti L., Leoni G., Scicchitano G. & Silenzi S. (2011) - *Sea level change along the Italian coast during the Holocene and projections for the future*. Quaternary International, 232 (1-2), 250-257. doi: 10.1016/j.quaint.2010.04.026.

Lambeck K., Antonioli F., Purcell A. & Silenzi S. (2004) - *Sea-level change along the Italian coast for the past 10,000 yr*. Quaternary Science Reviews, 23 (14-15), 1567-1598. doi: 10.1016/j.quascirev.2004.02.009.

Lericolais G., Auffret J.P. & Bourillet J.F. (2003) - *The Quaternary Channel River: Seismic stratigraphy of its palaeo-valleys and deeps*. Journal of Quaternary Science 18, 245-260. doi: 10.1002/jqs.759.

Lisco S., Corselli C., De Giosa F., Mastronuzzi G, Moretti M., Siniscalchi A., Marchese F., Bracchi V., Tessarolo C. & Tursi, A. (2016) - *Geological maps of a marine area polluted by industrial discharges (Mar Piccolo, Taranto, southern Italy): the physical basis for remediation*. Journal of Maps, 12 (1), 173-180.

Martinis B. & Robba E. (1971) - *Note illustrative della Carta Geologica d'Italia, F. 202 'Taranto'*. Servizio Geologico d'Italia, Arti Grafiche E. Di Mauro, Cava dei Tirreni, Italy, 56 pp.

Maselli V. & Trincardi F. (2013) - *Large-scale single incised valley from a small catchment basin on the western Adriatic margin (central Mediterranean Sea)*. Global and Planetary Change, 100, 245-262.

Mastronuzzi G. & Sanso' P. (1998) - *Morfologia e genesi delle Isole Chéradi e del Mar Grande (Taranto, Puglia, Italia)*. Geografia Fisica e Dinamica Quaternaria, 21, 131-138.

Mastronuzzi G. & Sansò P. (2003) - *Quaternary coastal morphology and sea level changes*. Field Guide. Puglia 2003, Final Conference – Project IGCP 437 UNESCO - IUGS, Otranto / Taranto - Puglia (Italy) 22- 28 September 2003, GI2S Coast – Gruppo Informale di Studi Costieri, Research Publication, 5, Brizio srl, Taranto,184 pp.

Mastronuzzi G., Boccardi L., Candela A.M., Colella C., Curci G., Giletti F., Milella M., Pignatelli C., Piscitelli A., Ricci F. & Sansò. P. (2013) - *Il Castello Aragonese di Taranto in 3D nell'evoluzione del paesaggio naturale*. Ed. DIGILABS, Bari, 171 pp.

Mele D., Sulpizio R., Dellino P. & La Volpe L. (2011) - *Stratigraphy and eruptive dynamics of a pulsating Plinian eruption of Somma-Vesuvius: The Pomici di Mercato (8900 years B.P.)*. Bulletin of Volcanology, 73(3), 257-278. doi: 10.1007/s00445-010-0407-2.

Mossa M. (2017) - http://www.michelemossa.it/stazionemeteo2.php.

Negri A., Amorosi A., Antonioli F., Bertini A., Florindo F., Lurcock P.C., Marabini S., Mastronuzzi G., Regattieri E., Rossi V., Scarponi D., Taviani M., Zanchetta G. & Vai G.B. (2015) - *A potential global boundary stratotype section and point (GSSP) for the Tarentian Stage, Upper Pleistocene, from the Taranto area (Italy): Results and future perspectives*. Quaternary International 383, 145-157.

Negri A., Florindo F., Lurcock P.C., Marabini S., Morigi C., Mastronuzzi G., Vetrone C. & Vai G.B. (2016) - *The Fronte candidate section for the Upper Pleistocene GSSP: a short report*. Alpine and Mediterranean Quaternary, 29 (2), 137-142.

Nordfjord S., Goff J.A., Austin J.A. & Sommerfield C.K. (2005) - *Seismic geomorphology of buried channel systems on the New Jersey outer shelf: assessing past environmental conditions*. Marine Geology 214, 339-364. doi: 10.1016/j.margeo.2004.10.035.

Pagliarulo R. & Bruno G. (1990) - *Implicazioni tettonico-strutturali nella circolazione idrica profonda nell'area del Mar Piccolo di Taranto (Puglia)*, Bollettino Società Geologica Italiana, 109, 307-312.

Parenzan P. (1960) - *Il Mar Piccolo di Taranto*. G. Semeraro Ed., Roma, 254 pp.

Parenzan P. (1972) - *L'anello di San Cataldo nel Mar Grande di Taranto*. Thalassia Salentina, *6*, 3-24.

Peirano A., Kružić P. & Mastronuzzi, P. (2009) - *Growth of Mediterranean reef of Cladocora caespitosa (L.) in the Late Quaternary and climate inferences*. Facies, 55, 325-333.

Peirano A., Morri C., Bianchi C.N., Aguirre J., Antonioli F., Calzetta G., Carobene L., Mastronuzzi G. & Orrù P. (2004) - *The Mediterranean coral Cladocora caespitosa; a proxy for past climate fluctuations?* Global and Planetary Change 40, 195-200.

Posamentier H.W. & Allen G.P. (1993) - *Variability of the sequence stratigraphic model: effects of local basin factors*. Sedimentary Geology 86, 91-109. doi: 10.1016/0037-0738(93)90135-R.

Posamentier H.W. (2001) - *Lowstand alluvial bypass systems: incised vs. unincised*. American Association of Petroleum Geologists Bulletin, 83, 1771-1793.

Posamentier, H. W. & Allen, G. P. (1993) - *Variability of the sequence stratigraphic model: effects of local basin factors*. Sedimentary Geology, 86 (1-2), 91-109.

Pouchou J.L. & Pichoir F. (1988) - *A simplified version of the "PAP" model for matrix corrections in EPMA, Microbeam Analysis*. In: Newbury D.E. (Ed.), Microbeam Analysis, San Fransisco Press, 315-318.

Pouchou J.L. & Pichoir F. (1991) - *Quantitative analysis of homogeneous or stratified microvolumes applying the model "PAP", Electron Probe Quantitation.* In: Heinrich K.F.J. & Newbury D.E. (Eds.), Electron Probe Quantitation. Plenum Press, New York, 31-75.

Rabineau M., Berné S., Ledrezen É., Lericolais G., Marsset T. & Rotunno M. (1998) - *3D architecture of lowstand and transgressive Quaternary sand bodies on the outer shelf of the Gulf of Lion, France.* Marine and Petroleum Geology 15, 439-452. doi: 10.1016/S0264-8172(98)00015-4.

Reijenstein H. M., Posamentier H. W. & Bhattacharya J. P. (2011) - *Seismic geomorphology and high-resolution seismic stratigraphy of inner-shelf and marine sequences, Gulf of Thailand*. AAPG bulletin, 95 (11), 1959-1990. doi: 10.1306/03151110134.

Reimer P.J., Bard E., Bayliss A., Beck J.W., Blackwell P.G., Bronk Ramsey C., Buck C.E., Cheng H., Edwards R.L., Friedrich M., Grootes P.M., Guilderson T.P., Haflidason H., Hajdas I., Hatté C., Heaton T.J., Hoffmann D.L., Hogg A.G., Hughen K.A., Kaiser K.F., Kromer B., Manning S.W., Niu M., Reimer R.W., Richards D.A., Scott E.M., Southon J.R., Staff R.A, Turney C.S.M. & Van der Plicht J. (2013) - *IntCal13 and Marine13 Radiocarbon Age Calibration Curves 0-50,000 Years cal BP.* Radiocarbon, 55, 4, 1869-1887.

Ricchetti G. (1967) - *Osservazioni preliminari sulla geologia e morfologia dei depositi quaternari nei dintorni del Mar Piccolo (Taranto)*. Atti Accademia Gioenia Scienze Naturali Catania, 6, 123-130.

Ricchetti G., Ciaranfi N., Luperto Sinni E., Mongelli F. & Pieri P. (1988) - *Geodinamica ed evoluzione sedimentaria e tettonica dell'Avampaese Apulo*. Memorie della Società Geologica Italiana, 41, 57-82.

Rossi V., Amorosi A., Sarti G. & Potenza M. (2011) - *Influence of inherited topography on the Holocene sedimentary evolution of coastal systems: An example from Arno coastal plain (Tuscany, Italy).* Geomorphology 135, 117-128. doi: 10.1016/j.geomorph.2011.08.009.

Santacroce R. & Sbrana A. (2003) - *Geological map of Vesuvius at the scale 1: 15,000.* SELCA ed., Florence.

Sarti G., Rossi V., Amorosi A., Bini M., Giacomelli S., Pappalardo M., Ribecai C., Ribolini A. & Sammartino I. (2015) - *Climatic signature of two mid-late Holocene fluvial incisions formed under sea-level highstand conditions (Pisa coastal plain, NW Tuscany, Italy).* Palaeogeography Palaeoclimatology Palaeoecology, 424, 183-195. doi: 10.1016/j.palaeo.2015.02.020.

Schwartz, M. [Ed.] (2005) - *Encyclopedia of coastal science*. Springer Science & Business Media.

Shackleton, N. J., (2000) - *The 100,000-year ice-age cycle identified and found to lag temperature, carbon dioxide, and orbital eccentricity.* Science, 289 (5486), 1897-1902.

Strong N. & Paola C. (2008) - *Valleys that never were: time surfaces versus stratigraphic surfaces*. Journal of Sedimentary Research 78, 579-593.

Stuiver M. & Polach H. A. (1977) - *Discussion reporting of 14 C data*. Radiocarbon, 19 (3), 355-363.

Stuiver M., Reimer P.J. & Reimer R.W. (2017) - CALIB 7.1 [WWW program] at http://calib.org.

Swift D.J.P. (1968) - *Coastal Erosion and Transgressive Stratigraphy*. The Journal of Geology, 76 (4), 444-456.

Tanabe S., Nakanishi T., Ishihara Y. & Nakashima R. (2015) - *Millennial-scale stratigraphy of a tide-dominated incised valley during the last 14 kyr: Spatial and quantitative reconstruction in the Tokyo Lowland, central Japan*. Sedimentology, 62, 1837-1872. doi: 10.1111/sed.12204.

Tesson M., Labaune C. & Gensous B. (2005) - *Small rivers contribution to the Quaternary evolution of a Mediterranean littoral system: the western gulf of Lion, France*. Marine Geology, 222, 313-334. doi: 10.1016/j.margeo.2005.06.021

Van Wagoner J.C., Posamentier H.W., Mitchum R.M., Vail P.R., Sarg R., Loutit T.S. & Hardenbol J. (1988) - *An overview of sequence stratigraphy and key definitions*. In: Wilgus, C.K., Hastings, B.S., Kendall, C.G.C., Posamentier, H.W., Ross, C.A., Van Wagoner, J.C. (Eds.), Sea-level Changes: An Integrated Approach. SEPM Special Publication, vol. 42. SEPM, Society for Sedimentary Geology, Tulsa, Oklahoma, USA, 39-45.

Verri A. & De Angelis D'ossat G. (1899) - *Cenni sulla geologia di Taranto*. Bollettino Società Geologica Italiana, XVIII, 2, 179-210.

Wilson G.P., Lamb A.L., Leng M.J., Gonzalez S. & Huddart D. (2005) - *Variability of organic $\delta^{13}C$ and C/N in the Mersey Estuary, U.K. and its implications for sea-level reconstruction studies*. Estuarine, Coastal and Shelf Science, 64, 685-698.

Zaitlin B.A., Dalrymple R.W. & Boyd R. (1994) - *The stratigraphic organization of incised-valley systems associated with relative sea-level change*. In: Dalrymple R.W., Boyd R., Zaitlin B.A. (Eds.), Incised-valley System: Origin and Sedimentary Sequences. SEPM Special Publication, vol. 51. SEPM, Society for Sedimentary Geology, Tulsa, Oklahoma, USA, 45-60.

Zecchin M. & Catuneanu O. (2013) - *High-resolution sequence stratigraphy of clastic shelves I: Units and bounding surfaces.* Marine and Petroleum Geology. 39, 1-25. doi: 10.1016/j.marpetgeo.2012.08.015.

Zecchin M., Ceramicola S., Gordini E., Deponte M. & Critelli S. (2011) - *Cliff overstep model and variability in the geometry of transgressive erosional surfaces in high-gradient shelves: The case of the Ionian Calabrian margin (southern Italy).* Marine Geology, 281 (1-4), 43-58. doi: 10.1016/j.margeo.2011.02.003.

Zuffianò L.E., Basso A., Casarano D., Dragone V., Limoni P.P., Romanazzi A., Santaloia F. & Polemio M. (2016) - *Coastal hydrogeological system of Mar Piccolo (Taranto, Italy)*. Environmental Science and Pollution Research, 23 (13), 12502-14. doi: 10.1007/s11356-015-4932-6.

(Ms. received 16 May 2017; accepted 25 June 2018)